Internal Inelastic Scattering Satellite Probed by Molecular-Frame Photoelectron Angular Distributions from CO_2

X.-J. Liu,[1] H. Fukuzawa,[1] T. Teranishi,[1] A. De Fanis,[1] M. Takahashi,[1] H. Yoshida,[2] A. Cassimi,[3] A. Czasch,[4] L. Schmidt,[4]
R. Dörner,[4] I. Koyano,[5] N. Saito,[6] and K. Ueda[1,*]

[1] *Institute of Multidisciplinary Research for Advanced Materials, Tohoku University, Sendai 980-8577, Japan*
[2] *Department of Physical Science, Hiroshima University, Higashi-Hiroshima 739-8526, Japan*
[3] *CIMAP CEA/CNRS/ENSICAEN, Box 5133, F-14070 Caen cedex 5, France*
[4] *Goethe-Universität Frankfurt am Main, Max-von-Laue-Str. 1, D-60438 Frankfurt, Germany*
[5] *Department of Material Science, Himeji Institute of Technology, Kamigori, Hyogo 678-1597, Japan*
[6] *National Metrology Institute of Japan, AIST, Tsukuba 305-8568, Japan*

(Received 20 February 2008; published 10 July 2008)

The molecular-frame photoelectron angular distribution (MFPAD) of the satellite accompanying the C 1s photoline of the CO_2 molecule has been measured at the C $1s(2\sigma_g) \rightarrow 4\sigma_u^*$ shape resonance, using electron-ion multicoincidence momentum spectroscopy. The observed MFPAD indicates that the conjugate satellite is excited by internal inelastic scattering. In this scenario, a photoelectron is ejected from the C $1s(2\sigma_g)$ orbital along the molecular axis and collides with an O lone-pair electron in the highest occupied molecular orbital $1\pi_g$. Then one of the colliding electrons is trapped to the lowest unoccupied molecular orbital $2\pi_u^*$, while the other is emitted as a satellite photoelectron of σ_g symmetry, losing the information of the original photoelectron emission direction and parity.

DOI: 10.1103/PhysRevLett.101.023001 PACS numbers: 33.60.+q, 33.80.−b, 34.80.−i

Electron correlations play a decisive role in the forming of the electronic structure and properties of atoms, molecules, and condensed matter. They also govern electronic processes such as photoexcitation or photoionization and the subsequent electronic decay. The simplest electronic process where electron correlations play an essential role is double photoionization of helium, which has for this reason been studied intensively by many researchers (see, for example, [1,2] and references therein.) Further clear evidence of electron correlations is the appearance of correlation satellites in photoelectron spectra; they appear as a signature of two-electron transitions accompanying a single photon ionization. Such correlation satellites in atomic photoionization have been extensively studied using synchrotron radiation (see, for example, [3] and references therein.) Correlation satellites in molecular photoelectron spectra also provide valuable information about electron correlations in molecules [4,5]. However the role of electron correlations in the molecular photoionization process has not been explored experimentally in as much detail as the corresponding processes in helium and other atoms. In the present work, we aim to elucidate the role of electron correlations in molecular photoionization. For this purpose, we investigate the molecular-frame photoelectron angular distribution (MFPAD) of a correlation satellite.

When considering molecular photoionization, the most natural reference frame is the molecular frame. The MFPADs for linear molecules can be realized by angle-resolved photoelectron-photoion coincidence measurements [6]. With the advent of position sensitive detectors, the measurement of MFPADs has become a standard procedure in molecular photoionization studies [7–14]. However, the measurements of MFPADs has so far been performed exclusively on the intense photoelectron mainlines.

We preface our discussion of correlation satellites with their phenomenological classification as well as classification based on satellite excitation mechanism. The satellites can be classified phenomenologically into two groups [15]. The first group includes satellites whose excitation cross sections relative to the single-hole ionization cross section stay relatively constant (the ‘‘normal’’ satellites), while the second group includes those satellites whose relative excitation cross sections sharply decrease with increasing photon energy (the ‘‘conjugate’’ satellites). These features are also seen in correlation satellites in molecular photoelectron spectra [16–19]. The different energy dependence for the normal and conjugate satellites stems from the fact that the final ionic states of the normal satellites have the same global quantum numbers as the mainline single-hole state, while those of conjugate satellites are different. For the K-shell photoionization of closed shell molecules with which we are concerned here, the angular momentum of the absorbed photon is carried away by the ejected electron both for the mainline and the normal satellites and is retained by the remaining ion for the conjugate satellites.

An alternative perspective is provided by a classification of correlation satellites based on the different lowest order diagrams of the many-body perturbation theory (MBPT) [3], as often discussed also for atomic double photoionization [2,20,21]. One of the two relevant contributions is termed ‘‘shake-up’’ while the other is termed ‘‘internal inelastic scattering’’ [3] or ‘‘two-step-one’’ (TS1)

[2,20,21]. The shake-up mechanism predominantly causes monopole excitation for the normal satellites and monopole ionization for the conjugate satellites. Replacement of the two-electron integral for the shake-up (in MBPT) by the overlap integral is known as the "shake-up model" [3,16,17]. It is worth noting that the monopole ionization term (conjugate shake-up term), also appears in the normal satellites and causes interference with the "direct (monopole excitation) term" [17]. In the internal inelastic scattering mechanism, on the other hand, multipole excitation becomes probable. Similarly to the shake-up mechanism, both normal and conjugate satellites may be excited by internal inelastic scattering. Thus, we have in total four different groups of correlation satellites, normal and conjugate satellites excited by shake-up and normal and conjugate satellites excited by internal inelastic scattering.

Normal and conjugate satellites excited by shake-up have previously been investigated in molecular photoionization both experimentally and theoretically (within the shake-up model) [16–19]. In these works the internal inelastic scattering mechanism was neglected. De Fanis *et al.* [22] and Hoshino *et al.* [23] on the other hand, suggest that internal inelastic scattering may also play a role in satellite excitation in molecules. The best way to investigate the mechanisms of the satellite excitation is to measure the MFPADs, since in this way one can probe not only the transition symmetry, i.e., which direction the *initial* photoelectron (before the internal inelastic scattering) is driven relative to the molecular axis, but also the symmetry of the *final* photoelectron wave (after the internal inelastic scattering). In the present work, we have investigated the MFPAD for the satellite in C 1s photoemission from carbon dioxide molecules CO_2, aiming to elucidate the mechanism of the satellite excitation. We show that the observed $\pi - \pi^*$ satellite, labeled $S4$ and assigned as a conjugate satellite by Schmidbauer *et al.* [24], is an example of a conjugate satellite excited by internal inelastic scattering.

The experiment was carried out on the c branch of the soft x-ray photochemistry beam line 27SU [25–27] at SPring-8. Our coincidence apparatus is based on the measurement of electron and ion times of flight (TOF) using two multihit two-dimensional position sensitive detectors [12,13], and is equivalent to cold-target recoil momentum spectroscopy or the reaction microscope [28]. Details of the setup and experimental procedures are given elsewhere [12,13,22]. A vertical supersonic jet of CO_2 crosses the horizontal photon beam. The TOF axis is in the horizontal direction and perpendicular to both the gas and photon beams. Ions are accelerated by a uniform electrostatic field to a detector at one end of the acceleration region while the same field accelerates electrons in the opposite direction where they enter a drift region. Each detector is fitted with a two-dimensional (2D) multihit readout delayline anode (Roentdek). This permits measurements of both time of detection and 2D position coordinates, thus allowing us to extract three-dimensional (3D) momentum. The orientation of the molecular axis at the time of photoemission is extracted from the momentum vectors of the CO^+ and O^+ fragments resulting from Coulomb dissociation of CO_2^{2+} subsequent to rapid Auger decay. The coincidence measurements were performed at the shape resonance energy ~312 eV.

In the analysis of the experimental data we have employed the projection method [29,30]. In this method, all possible experimental information is encapsulated in four one-dimensional (1D) functions. With these functions we can reconstruct MFPADs for any angles between the molecular axis and the E vector [31]. Since we use all the data points to obtain only four 1D functions by this method, the statistics in the data analysis are far improved compared to the conventional approach where the reaction plane is predefined [12]. This improvement has allowed us to extract the MFPAD for the weak satellite with good statistics.

The ground state electron configuration of CO_2 is

$$1\sigma_g^2 1\sigma_u^2 2\sigma_g^2 3\sigma_g^2 2\sigma_u^2 4\sigma_g^2 3\sigma_u^2 1\pi_u^4 1\pi_g^4;$$
$$2\pi_u^{*0} 5\sigma_g^{*0} 4\sigma_u^{*0} X^1\Sigma^+,$$

where $1\sigma_g$ and $1\sigma_u$ denote O 1s core orbitals and $2\sigma_g$ denotes C 1s. The highest occupied molecular orbital (HOMO) is the O 2p lone-pair orbital. In the C K-shell absorption spectrum of CO_2, one can see one sharp strong resonance corresponding to promotion of the $2\sigma_g$ electron to the lowest unoccupied molecular orbital (LUMO) $2\pi_u^*$ below the C 1s ionization threshold, and one broad resonance corresponding to $2\sigma_g \rightarrow 4\sigma_u^*$ promotion above the threshold. The latter is the shape resonance. A promotion of the $2\sigma_g$ electron to $5\sigma_g^*$ is dipole forbidden. The photon energy employed in the present experiment corresponds to the $2\sigma_g \rightarrow 4\sigma_u^*$ shape resonance.

Figure 1 shows an electron spectrum recorded at a photon energy of 311.8 eV, i.e., ~14.2 eV above the C 1s threshold at 297.63 eV [32]. Besides the mainline we can see the satellite at a binding energy of ~11.5 eV relative to the mainline. This satellite band corresponds to the overlapping bands $S1$ and $S4$, assigned, respectively, to normal and conjugate satellites by Schmidbauer *et al.* [24], based on the photon energy dependence of the excitation cross sections. In order to determine the MFPADs of the

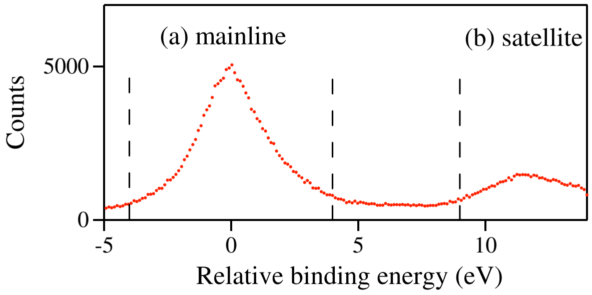

FIG. 1 (color online). C 1s photoelectron spectrum of CO_2 recorded at 311.8 eV.

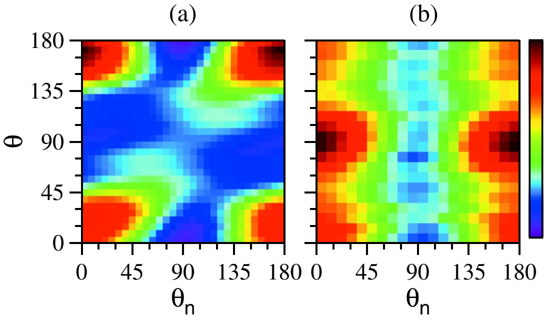

FIG. 2 (color online). 2D plots of MFPADs for (a) the C 1*s* main line and (b) the lowest satellite of CO_2 recorded at photon energy of 311.8 eV. The *x* axis denotes the angle θ_n between the *E* vector and molecular axis, and the *y* axis the electron emission polar angle θ relative to the molecular axis. The electron emission intensity is plotted on a gray linear scale (color scale). These distributions have not been directly measured, but reconstructed from a parametrization of all available MFPADs for various molecular orientations. See text for details.

mainline and the unresolved satellite bands, shown in Figs. 2(a) and 2(b), we select the reaction geometry such that the electron is emitted in the plane defined by the molecular axis and the *E* vector. In both cases, the electron emission is enhanced when the molecule is aligned along the *E* vector ($\theta_n \sim 0°$ and $\sim 180°$). The three-dimensional MFPADs for the mainline and the satellite band are shown in Figs. 3(a) and 3(b), where the *E* vector is parallel to the molecular axis ($\theta_n = 0°$).

Let us first consider the C 1*s* ($2\sigma_g$) mainline. Since the excitation energy is close to the peak of the $2\sigma_g \rightarrow 4\sigma_u^*$ shape resonance, the final state is expected to be able to be described as $2\sigma_g^{-1}(^2\Sigma_g^+)4\sigma_u^*\ {}^1\Sigma_u^+$. This $\Sigma_g \rightarrow \Sigma_u$ photoexcitation is a parallel transition, and the ejected photoelectron has predominantly σ_u symmetry. From Figs. 2(a) and 3(a) it is clear that the mainline photoemission proceeds mostly along the molecular axis ($\theta \sim 0°$ and $\sim 180°$) when the molecule is aligned along the *E* vector ($\theta_n \sim 0°$ and $\sim 180°$). This is consistent with the expectation that the $2\sigma_g \rightarrow 4\sigma_u^*$ shape resonance is a $\Sigma_g \rightarrow \Sigma_u$ parallel transition and that the ejected photoelectron has σ_u symmetry with a node at $\theta = 90°$ [Figs. 2(a) and 3(a)].

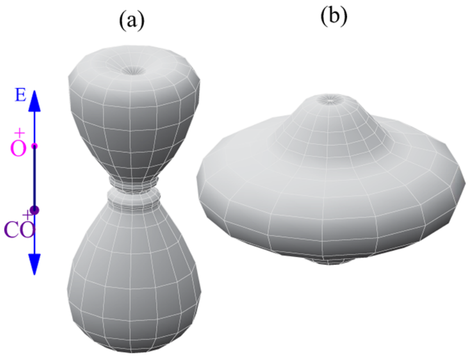

FIG. 3 (color online). 3D plots of MFPADs for (a) the C 1*s* main line and (b) the lowest satellite of CO_2 recorded at photon energy of 311.8 eV, where the *E* vector is parallel to the molecular axis. These distributions have not been directly measured but instead have been reconstructed from a parametrization of all available MFPADs for various molecular orientations. See text for the details.

Let us now focus on the satellite with the intent of assigning it to one of the four types described in the introduction. From Fig. 2(b) it is clear that the satellite photoemission is enhanced when the molecule is aligned along the *E* vector, revealing the predominance of the $\Sigma_g \rightarrow \Sigma_u$ parallel transition, as in the case of the mainline. Thus the global quantum number of the continuum state that consists of the ion and the photoelectron is Σ_u. If it were a normal satellite, then the global quantum number of the ion state would be $^2\Sigma_g^+$ because the mainline (single-hole) state is $2\sigma_g^{-1}\,{}^2\Sigma_g^+$. Then, the detected electron would be σ_u, giving a node at $\theta = 90°$ in the MFPAD, as for the mainline. However, the MFPAD for the satellite clearly shows maximum intensity at $\theta = 90°$ [Figs. 2(b) and 3(b). Thus the observed satellite is predominantly a conjugate satellite, as Schmidbauer *et al.* suggested for the *S*4 band [24]. The electron emission parallel to the molecular axis seen in Figs. 2(b) and 3(b) may reflect the contribution from the normal satellite *S*1.

Next we turn to the question of the excitation mechanism. For a conjugate satellite excited by shake-up (within the shake model), the *dipole* excitation of the core electron to an unoccupied molecular orbital (bound-bound dipole integral) is accompanied by the *monopole* ionization of the valence electron (bound-free overlap integral). If the observed C 1*s* ($2\sigma_g$) satellite is caused by this conjugate shake-up term, the $2\sigma_g$ electron is promoted to the LUMO $2\pi_u^*$ via dipole excitation (since this transition moment is by far larger than any other), and one valence electron is shaken off via the monopole transition. In this case, the photoexcitation is a $\Sigma_g \rightarrow \Pi_u$ perpendicular transition. However, as already noted, the satellite excitation is enhanced by the $\Sigma_g \rightarrow \Sigma_u$ parallel transition. Thus the observed conjugate satellite is not excited by shake-up.

Let us now examine whether the observed satellite is consistent with the prediction for internal inelastic scattering. In this scenario, the photoelectron interacts with the valence electron and exchanges momentum. Schmidbauer *et al.* [24] suggest an assignment of $2\sigma_g^{-1}1\pi_u^{-1}2\pi_u^*\Sigma_g^-$ or Δ_g for the *S*4 conjugate satellite. Our observation rejects this assignment because one cannot construct a Σ_u continuum state adding a photoelectron that has a maximum intensity distribution at $\theta = 90°$ to the ion. An alternative plausible assignment is $2\sigma_g^{-1}1\pi_g^{-1}2\pi_u^*$. Adding a σ_g photoelectron to this ion, it is possible to construct a Σ_u continuum state. The observed MFPAD shown in Figs. 2(b) and 3(b) agrees with the σ_g symmetry. Also, internal inelastic scattering between the photoelectron and the valence electron in a π_g HOMO with O 2*p* lone-pair character is expected to be enhanced when the initial photoelectron current ejected from the central C is towards the O atom, i.e., for the $\Sigma_g \rightarrow \Sigma_u$ parallel transition. Thus, all of our observations, i.e., that the satellite emission intensity is highest for a parallel transition and that the satellite MFPAD is peaked perpendicular to the molecular axis, strongly support classification as a conjugate satellite excited by internal inelastic scattering, with the assignment of the remaining ion $2\sigma_g^{-1}1\pi_g^{-1}2\pi_u^*$.

It is worth noting that, while the mainline MFPAD [Fig. 2(a)] changes dramatically with the excitation angle θ_n, the shape of the satellite MFPAD [Fig. 2(b)] is more or less constant, with only the total intensity changing with θ_n. Such a total "loss of memory" of the photoelectron emission direction in the satellite production is also consistent with classification as a conjugate satellite excited by internal inelastic scattering. As noted above, the photoelectron collides with the O $2p1\pi_g$ lone-pair electron. To describe this electron-electron collision, two two-electron matrix elements, $\langle \epsilon' \sigma_g 2\pi_u | \frac{1}{r_{12}} | \epsilon \sigma_u 1\pi_g \rangle$ and $\langle \epsilon' \sigma_g 2\pi_u | \frac{1}{r_{12}} | 1\pi_g \epsilon \sigma_u \rangle$ are involved. The former represents the process that the O $2p1\pi_g$ electron is promoted to $2\pi_u$ and the photoelectron loses energy and appears as the satellite photoemission, changing its parity. The latter represents the process that the original photoelectron is trapped to $2\pi_u$, and the O $2p1\pi_g$ electron is ejected as the satellite photoemission. Because of the two-step collision governed by these two matrix elements, the photoelectron loses its memory of the original photoelectron emission direction and parity. We cannot, however, exclude the possibility that PCI between the low energy satellite electron and the Auger electron may also play a role in the loss of memory.

We speculate that the shape resonance plays a key role for the enhancement of this satellite. The initial photocurrent is enhanced by the $2\sigma_g \rightarrow 4\sigma_u^*$ shape resonance, whereas the satellite may be enhanced also by the $5\sigma_g^*$ shape resonance because the kinetic energy of the satellite (~ 2.5 eV) is close to the expected $5\sigma_g^*$ shape resonance energy. This double resonance structure may explain the strong enhancement of the satellite excitation by internal inelastic scattering, which is otherwise usually weak.

In summary, we have shown that the measurement of MFPADs using electron-ion multicoincidence momentum spectroscopy is a powerful tool to label the mechanisms of satellite excitation. Namely, we have found that the satellite accompanying the C 1s photoline of the CO_2 molecule is enhanced in the direction perpendicular to the molecular axis when the molecule is parallel to the electric vector of the incident radiation. This finding accommodates well with the scenario that a conjugate satellite is excited by internal inelastic scattering between one of the $1\pi_g$ valence electrons and the C 1s photoelectron of σ_u symmetry. In this scenario, one of the two colliding electrons fill the $2\pi_u^*$ LUMO while the other is ejected as a satellite photoelectron of σ_g symmetry, losing its memory of the original photoelectron emission direction and parity. We note that the present interpretation has been made within the dipole approximation. Further refined theoretical studies are desired in the future.

This experiment was carried out with the approval of JASRI and supported in part by Grants-in-Aid for Scientific Research from the Japan Society for the Promotion of Science (JSPS). The authors are grateful to A. Grum-Grzhimailo and M. Ehara for discussion and J. Harries for critical reading. X. J. L. and A. D. acknowledge financial support from JSPS. A. C. and R. D. acknowledge support by DFG.

*Corresponding author.
ueda@tagen.tohoku.ac.jp

[1] J. Briggs and V. Schmidt, J. Phys. B **33**, R1 (2000).
[2] J. H. McGuire, *Electron Correlation Dynamics in Atomic Collisions* (Cambridge University Press, New York, 2005) Chap. 7.
[3] V. Schmidt, Rep. Prog. Phys. **55**, 1483 (1992).
[4] L. S. Cederbaum *et al.*, Adv. Chem. Phys. **65**, 115 (1986).
[5] A. D. O. Bawagan and E. R. Davidson, Adv. Chem. Phys. **110**, 215 (1999).
[6] E. Shigemasa *et al.*, Phys. Rev. Lett. **74**, 359 (1995).
[7] F. Heiser *et al.*, Phys. Rev. Lett. **79**, 2435 (1997).
[8] A. Lafosse *et al.*, Phys. Rev. Lett. **84**, 5987 (2000).
[9] Y. Hikosaka and J. H. D. Eland, J. Phys. B **33**, 3137 (2000).
[10] A. Landers *et al.*, Phys. Rev. Lett. **87**, 013002 (2001).
[11] T. Jahnke *et al.*, Phys. Rev. Lett. **88**, 073002 (2002).
[12] N. Saito *et al.*, J. Phys. B **36**, L25 (2003).
[13] N. Saito *et al.*, J. Phys. B **38**, L277 (2005).
[14] J. Adachi *et al.*, J. Phys. B **40**, F285 (2007).
[15] U. Becker and D. A. Schirley, Phys. Scr. **T31**, 56 (1990).
[16] L. Ungier and T. D. Thomas, Phys. Rev. Lett. **53**, 435 (1984).
[17] J. Schirmer *et al.*,Phys. Rev. A **44**, 5762 (1991).
[18] K. Ueda *et al.*, Phys. Rev. Lett. **94**, 243004 (2005).
[19] M. Ehara *et al.*, J. Chem. Phys. **124**, 124311 (2006).
[20] A. Kheifets, J. Phys. B **34**, L247 (2001).
[21] A. Knapp *et al.*, Phys. Rev. Lett. **89**, 033004 (2002).
[22] A. De Fanis *et al.*, Phys. Rev. Lett. **89**, 023006 (2002).
[23] M. Hoshino *et al.*, J. Phys. B **36**, L381 (2003)
[24] M. Schmidbauer *et al.*, Phys. Rev. A **52**, 2095 (1995).
[25] H. Ohashi *et al.*, Nucl. Instrum. Methods Phys. Res., Sect. A **467-468**, 529 (2001).
[26] H. Ohashi *et al.*, Nucl. Instrum. Methods Phys. Res., Sect. A **467-468**, 533 (2001).
[27] K. Ueda, J. Phys. B **36**, R1 (2003).
[28] J. Ullrich *et al.*, Rep. Prog. Phys. **66**, 1463 (2003).
[29] R. R. Lucchese *et al.*, J. Electron Spectrosc. Relat. Phenom. **155**, 95 (2007).
[30] X.-J. Liu *et al.*, J. Phys. B **40**, 485 (2007).
[31] R. R. Lucchese *et al.*, Phys. Rev. A **65**, 020702(R) (2002).
[32] K. C. Prince *et al.*, J. Phys. B **32**, 2551 (1999).